2011-08

Time progression of ultrashort laser ablation in a transparent material

Laser Physics, Moscow : M A I K Nauka - Interperiodica, v. 21, n. 8, p. 1420-1427, Aug. 2011
http://www.producao.usp.br/handle/BDPI/50119

ISSN 1054-660X, Laser Physics

Time Progression of Ultrashort Laser Ablation in a Transparent Material[1]

G. Nicolodelli*, R. F. Z. Lizarelli, M. M. Costa***, and V. S. Bagnato******

Physics Institute of São Carlos, USP, São Carlos, SP, Brasil
Instituto de Física de São Carlos – USP/Grupo de Óptica, Av. Trabalhador Sancarlense, 400 Caixa Postal: 369 São Carlos CEP: 13560-970, Brasil
*e-mail: nicolodelli@ursa.ifsc.usp.br
**e-mail: lizarelli@if.sc.usp.br
***e-mail: mardo.abc@gmail.com.
****e-mail: vander@if.sc.usp.br

Received December 21, 2010; in final form, February 17, 2011; published online July 4, 2011

Abstract—Laser ablation on the ultra-short-pulses regime (femtosecond), has an impact on materials processing and micromachining in a quite profound ways. The investigation of the time progression of the laser ablation process within the material can produce much information and it is not conventionally used. The implementation of such study is the main aim of this paper. The temporal dependence of the diameter and depth of micro-drilling in the sample was verified, beyond the simple understanding of the mechanism for plasma generated during the ablation. From the monitoring of the time progression of the ablation, the time dependence for the velocity of ablation had been determined. In most cases, fume attenuation of the incoming laser beam and fume escape paths, produce dominant influence the characteristics of the region ablated. The method here employed is simple and can be carried out in real time without interruption of the process. In the implemented method light scattered from an auxiliary source allow visualization and record of the ablated geometry as it progress.

DOI: 10.1134/S1054660X11150187

INTRODUCTION

The use of ultrafast laser pulses is having an impact on materials and processing in biological tissues in a profound ways [1–7]. Laser precision engineering is being extensively applied in industries for device micro-fabrication due to its unique advantages of being a dry and noncontact process, coupled with the availability of reliable light sources and affordable system cost [8, 9]. New methods have been studied to improve the laser processing on materials [9, 10] and in hard tissues [2, 7, 11]. Femtosecond laser processing is useful for micromachining of materials to fabricate micro- and nano-structured devices, where high spatial resolution and reduced thermal damage are required [12, 13]. This is achieved due to the ultrashort time interaction between the laser pulse and the material [14]. Femtosecond lasers, operating at single photon energies far below the material bandgap energy, allow volumetric processing to a depth limited only by the working distance of the focusing element [15].

Interaction of ultra-short laser pulses with transparent materials has attracted much interest since the advent of powerful femtosecond lasers [16–18]. When femtosecond laser pulses are tightly focused within a transparent bulk material, nonlinear absorption can be induced in the focal volume and lead to highly localized energy deposition resulting in a range of possible changes in material properties [19]. Three-dimensional micromachining of optical materials is an important technique in various fields, such as telecommunications and biomedical technologies [20].

Recently, this technology has been employed to fabricate photonic structures in polymer [19], opening up doors for many applications due to their adjustable properties. In the past, PMMA (Polymethyl methacrylate) has been studied extensively with respect, to fs-laser machining [21], due to facility to include dopants as well from the fact that it presents high transmission in the visible region [20]. In particular, PMMA is an inexpensive and widely used polymer and it is the color of communications-grade polymer optical fibers [15]. In ophthalmology, PMMA is used for the fabrication of optical components and intraocular lenses (IOLs) due to its biocompability, lightness, flexibility, and easy formability [22] and therefore its characteristics under femtosecond laser ablation are intrinsically important.

The surface structures typically produced cavities and bumps are strongly related to the thermal effects of vaporization due to thermal diffusion, interaction with the hot vapor plume, and the low-energy-density region in the laser pulse. These effects produce undesired thermal damage around the processed complex structure. In order to produce a clean, well-defined

[1] The article is published in the original.

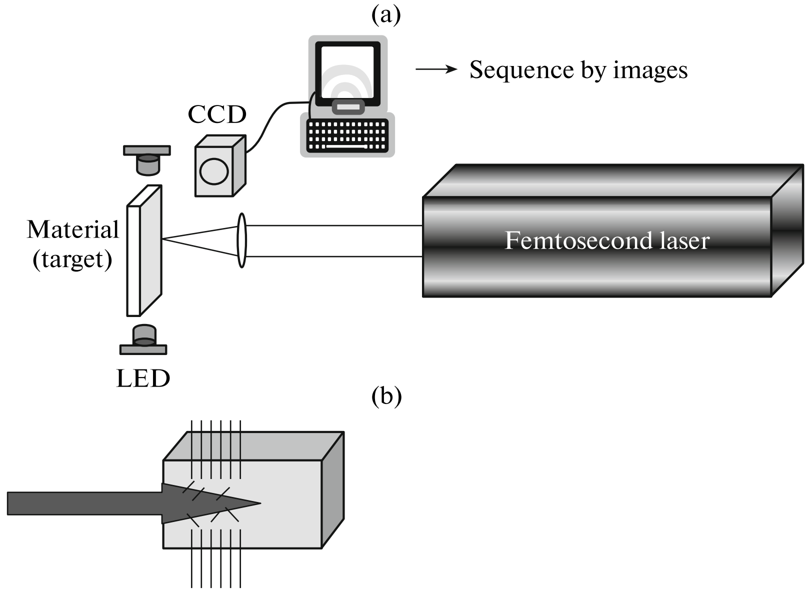

Fig. 1. (a) Experimental setup for obtain the temporal ablation motoring and (b) the scattering light in the sample.

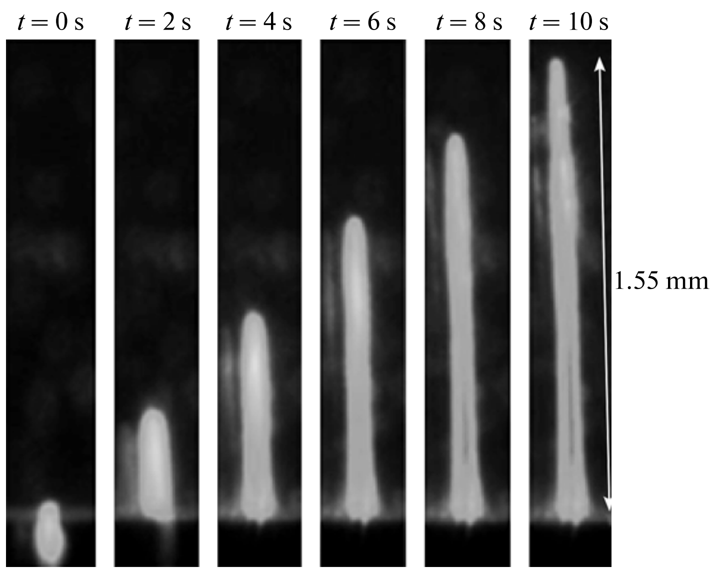

Fig. 2. Sequence of optical images obtained during the temporal ablation process of PMMA.

structure, several methods for reducing thermal damage and debris have been proposed [23]. Laser ablation in water, in vacuum, and at the rear surface provides very smooth edges and cavity reduced debris [14].

Due to the high peak powers available from such lasers, the peak intensity of the pulse focused can be extremely high, thus inducing nonlinear optical processes such as nonlinear multi-photon absorption [22]. Nonlinear excitation can lead to physical processes such as avalanche ionization, electron plasma formation and shock wave-induced micro-explosions [24]. Consequently, materials which are normally transparent to the infrared light (IR) such as PMMA can be efficiently ablated using femtosecond pulses of infrared light [22]. In summary, the benefits of this technique include the focused ability of near-infrared femtosecond laser pulses to induce localized structural change in transparent materials by nonlinear absorption while minimizing the influence of heat to the surrounding areas.

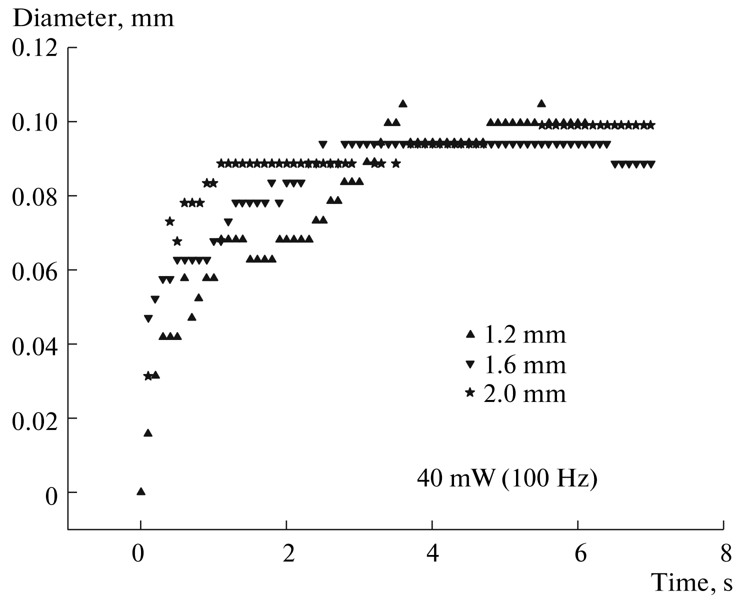

Fig. 3. Graphic of the dependence of ablated diameter as a function of time for a repetition rate of 100 Hz.

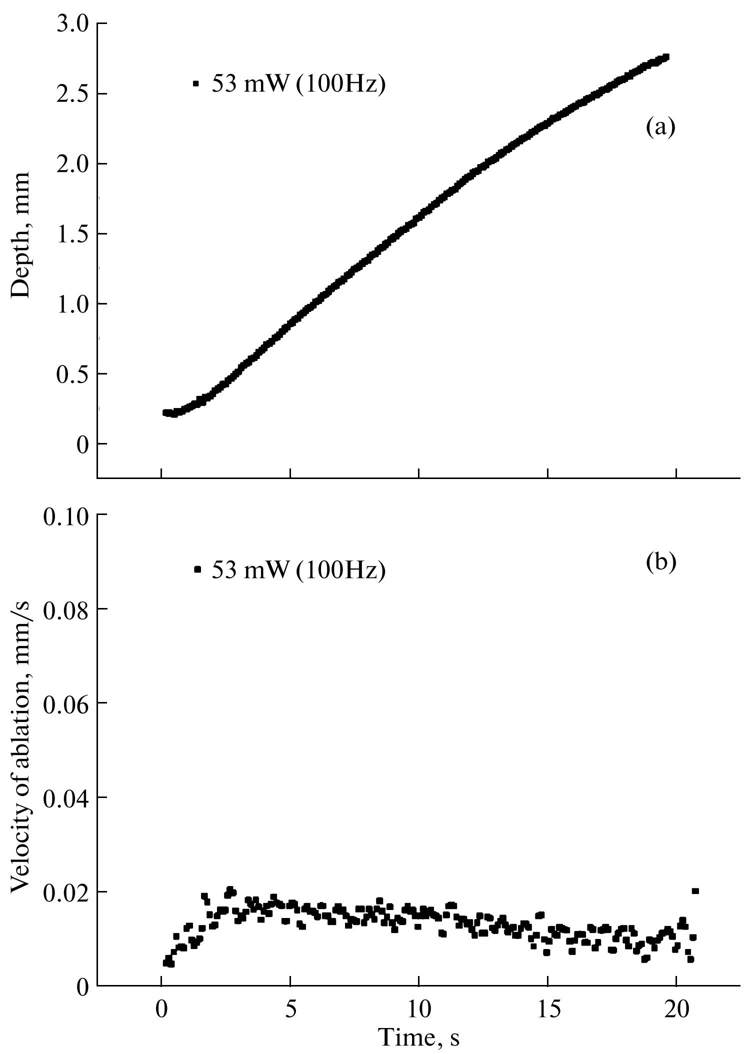

Fig. 4. (a) Graphic of the dependence of ablated depth as a function of time for a repetition rate of 100 Hz and (b) the dependence of velocity as a function of time.

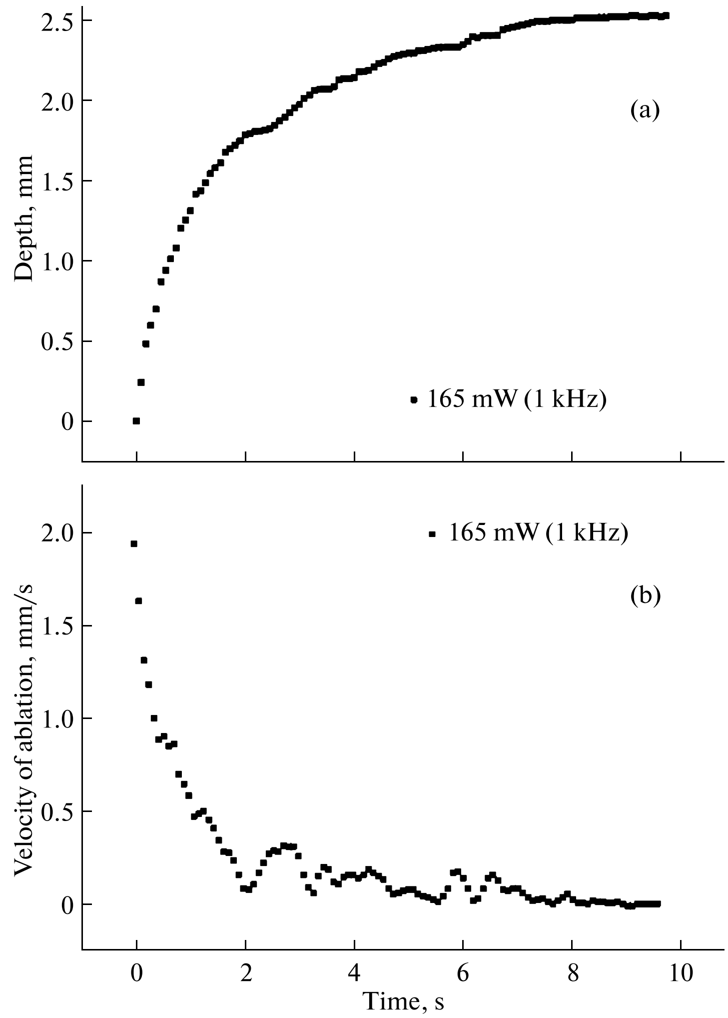

Fig. 5. (a) Graphic of the dependence of ablated depth as a function of time for a repetition rate of 1 kHz and (b) the dependence of velocity as a function of time.

The speed of laser ablation is a decisive factor in microsurgery and laser micro-fabrication. Model description of the propagation of the light into the dielectric sample has been proposed by Christensen and Balling [25]. Other studies describe the rate of ablation in PMMA [22] and hard tissues [26] using established laser parameters. Rajesh and Bellouard shown in their study the energy deposited as a function of the writing speed for different repetition rates, in fused silica [27]. So far, there is no report in the literature concerning the monitoring of the ablation speed processing in transparent material. The main aim of our study was to monitor the speed of temporal ablation in transparent dielectric materials. In addition, this study aims to add new understanding to the mechanisms responsible for the aberrations caused on the inner walls of the ablated cavities. Those studies may add important insights for future applications.

MATERIALS AND METHODS

A Ti:sapphire femtosecond (Pound-O, Coherent, Palo Alto, CA, USA) laser, emitting pulses of 70 fs, approximately, at wavelength of 801 nm, operating at a maximum pulse repetition rate of 1 kHz, was used in this study. Pulse duration of 70 fs was measured using 2nd—order auto-correlator (Coherent-SSATM, USA).

Pulse energy was attenuated by half-wave plate and the exposure time was controlled by a mechanic shutter. We have performed experiment using PMMA bulk samples ($40 \times 14 \times 8$ mm^3), and six surfaces of the sample were polished. Sample was mounted on a manually controlled *xyz* translation stage. The beam was steered using highly reflective dielectric mirrors and passed through a 20 cm focal length lens before reaching the target sample. The experimental optical set up resulted in a Gaussian laser beam of a waist "ω_0" of around 17

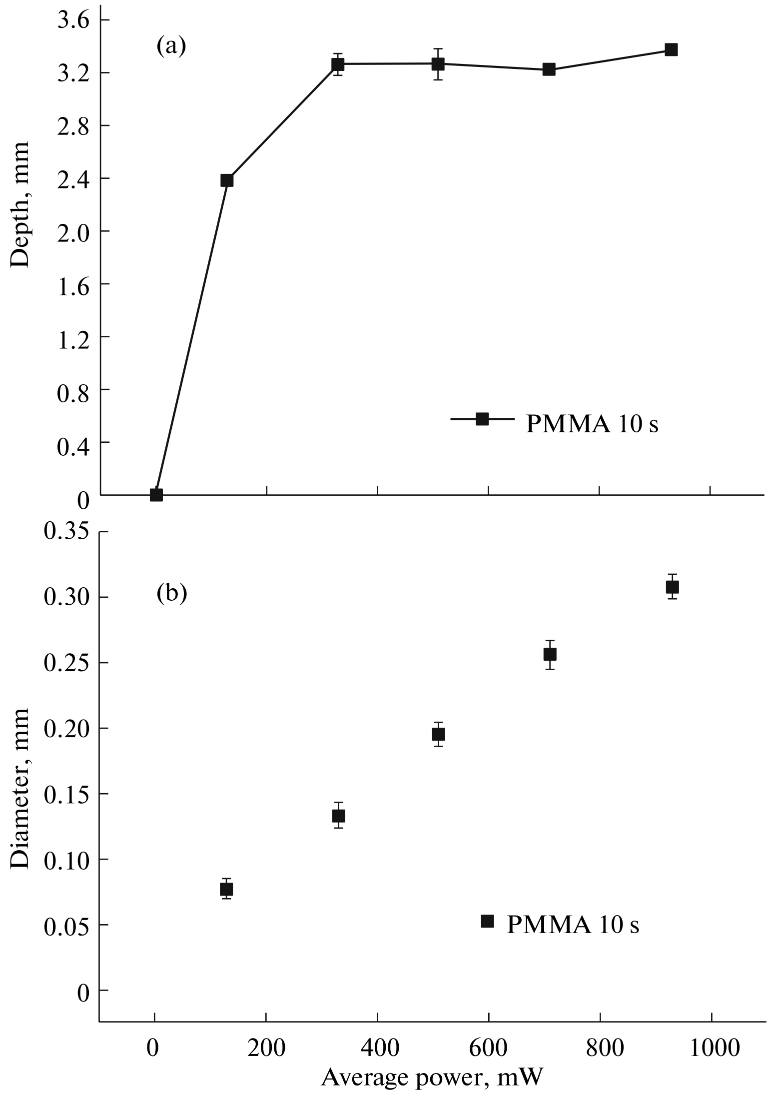

Fig. 6. Graphs considering behavior of the depth (a) and surface diameter (b) of ablation, as a function of the average power, when PMMA has been irradiated.

μm at the focal point. The technique used was the percussion method, when a sequence of laser pulses is directly focused on the surface of the target, resulting in the material ablation and consequently the production of a hole [9]. Laser pulses propagated along the optical axis (+*z* direction). The transparent target (PMMA) was vertically irradiated with two LEDs (Light Emitting Diodes) (*x* direction). A CCD (charge-coupled device) camera (attached to an imaging lens) was used placed on the y direction. A computer collects the optical image sequences of structural change. LEDs were used to improve the quality images and using filters and mirrors we have blocked almost all scattered light of IR (infrared) laser irradiation. Light from the LEDs are scattered by the ablated region allowing very good images.

At Fig. 1 the overall experimental set up is shown. Figure 1b shows details of the scattering of light, revealing the ablated geometry.

The PMMA samples were differently irradiated at average power levels ranging 0.1 to 1.0 W. Energy per pulse <1 mJ and exposure times (10 to 15 s). Surface of the sample was placed at focus.

In the first experiment, the temporal dependence of the diameter and depth of micro-drilling was verified in the sample. The experiment consists in the determination of the ablation speed, from the monitoring of the progression of the ablation with time. The sequences of the images were obtained simultaneously with the ablation process of the material through a CCD camera. Dimension can be directly obtained from images through a Matlab routine. In a second experiment, digital images of the micro-cavities were

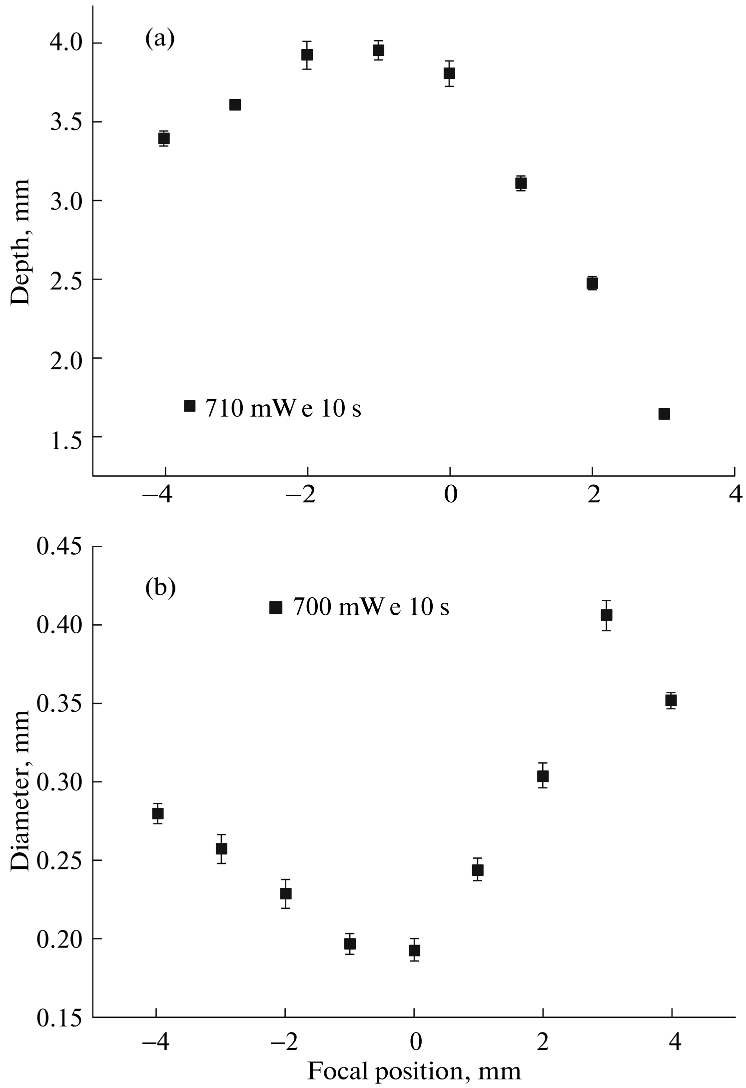

Fig. 7. Graphs considering behavior of the depth (a) and surface diameter (b) of ablation, as a function of the focus length, when PMMA has been irradiated.

obtained using a CCD camera attached to the optical microscope. From this image we have analyzed the geometry of the ablated micro-cavity.

RESULTS AND DISCUSSION

At Fig. 2 we show a sequence of shots revealing the temporal progression for the micro-channel during the process. For this case, energy per pulse of 500 μJ was used in a repetition rate of 100 Hz. For the image at $t = 0$, we observe the scattering of light out of the material, caused by the strong plasma ejected. That is severally suppressed after the bulk ablation starts to take place. This represents an example of data obtained.

The graphic presented at Fig. 3, shows a study of the diameter of the ablated hole for different depths ($z = 1.2$, 1.6, and 2.0 mm) as a function of time. For this specific experiment the energy per pulse of 400 μJ was used in a repetition rate of 100 Hz. For all positions, the increase of diameter as time goes by is observed. Interesting to observe that deeper in the rate of growth for the diameter with time is larger when compared to depth close to the surface. This effect is called "barrel effect," where the plasma blinding occurs into material resulting in an increase of the volume ablated. It is however interesting to note that at larges times the steady state is such that farther from the incident surface (z_0) smaller is the final diameter, showing that the configuration turn to a "cone geometry."

The dependence of depth of ablation as a function of time is the show at Fig. 4a. In this experiment an average power of 53 mW was used in a repetition rate of 100 Hz. That corresponds to energy per pulse of 530 μJ. From this data we have determinate the velocity of ablation progression into material as a function of the irradiation time (Fig. 4b).

While the ablation first increases the speed, at about 2.5 s the maximum is reached starting a slowdown after that. This behavior is a result from the laser beam geometry and the capacity of the material to be ejected. A shielding effect is believed to decrease the progression velocity. In this case, the longer duration of irradiation imply an accumulation of pulse, and therefore it take a heating of the ejected material and consequently of the plasma. A second effect contributing to the slowdown in velocity came from the defocusing of the laser as it go deep inn.

At Fig. 5a we show the dependence of depth of ablation as a function of time for an average power of 165 mW and a repetition rate of 1 kHz. The corresponding velocity of ablation into material as a function of the irradiation time is presented at Fig. 5b. Increasing power and repetition rate the behavior is quite different. The depth of ablation grows until it tends to a maximum value of approximately 2.5 mm. It occurs due to this limitation of the Gaussian beam focus used in this experiment. Femtosecond lasers allow volumetric processing to a depth limited by the working distance of the focusing element [15]. At Fig. 5b, we observed that the velocity of ablation decreases exponentially as time passes, tending to zero. The limitation distance around 2 mm is associated with the beam characteristic. Our beam has a Rayleigh parameter of 1.1 mm calculated from the focus waist data ($\omega_0 = 17$ μm). Thus, out of focal position, mechanisms as shockwave are the responsible for material cavitations, decreasing the efficiency of ablation. The occurrences of non-linear absorption and other of optic-mechanical character also are taking place. These effects must influence the ablation threshold and depth of micro holes. The dominant limitation is believed to be the focus of the used lens.

Figure 6 shows the behavior of the maximum depth of cavities and diameter of cavities at the entrance surface, when we have changed average power (or the laser fluence) irradiation of surface of samples of PMMA using femtosecond laser using 1 kHz of repetition rate. While the depth saturates at the higher power (Fig. 6a), the diameter (Fig. 6b) shows a monotonic growth with average power. This is a clear indication of limitation present in the longitudinal progression which is not present at surface.

Chapping the focus position the maximum obtained depth and surface diameter are shown at Figs. 7a and 7b. While the beam is incident convergent or divergent at the sample different depth of ablation is obtained as expected. However, it is interesting the asymmetric behavior of the surface ablated diameter around the focus. This behavior (Fib. 7b) suggest much more than geometry factors going on during the ablation.

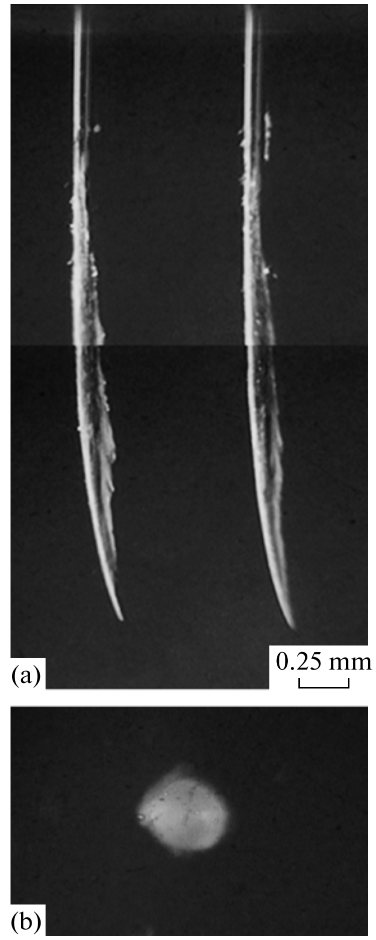

Fig. 8. Micro-cavities resulting image of femtosecond laser ablation in PMMA using 330 mW average power, 1 kHz repetition rate and 10 s of exposition time, cavity profile (a) and surface diameter (b).

The micro-cavities resulting image of femtosecond laser ablation in PMMA using 330 mW of average power, 1 kHz repetition rate and 10 s of exposition time are shown at Fig. 8.

PMMA may shows, at random, defects in its microstructure. These defects associated with attenuation effects along the way that the laser beam goes through within the material and can change the type of interaction mechanism, generating heat and subproducts, such as vapor, along the cavity.

Considerations from Canestri [28] allow observe what it occurs in cavity profile at Fig. 8. The heat of the plume of ablation may be responsible for changing the shape of the cavity, which in this case, according to the observed sample of PMMA. At Fig. 8, it hasn't a perfectly conical shape. The curvature inside the cavity occurred on the opposite side of the surface irregularity. This may be due to processes of fluid turbulence inside the cavity to displace laterally the hot steam of the ablated material during his exit, promoting the area median, a deposition of ablated material. Then, the deposition occurs laterally in the cavity walls, promoting an increase of strong turbulent processes in these areas, and this would result in the formation of a curvature of the cavity. Fume or smoke attenuation of the incoming laser beam, smoke exhaust paths, internal beam interference phenomena, blinding per plasma, media's micro-structural changes and, perhaps more importantly, their combination can offer good described explanations of all the phenomena.

CONCLUSION

In this paper, we report dynamic beam progression of ultrashort laser ablation in transparent dielectric materials using femtosecond laser pulses. From the time monitoring of the progression of the ablation, the ablation speed is determined. Due to the importance of femtosecond micromachining applications the development of techniques that allow a real time follow up is important. The time dependence of the ablation progression and its velocity allow infer about effects that can cause limitations on the ablation rate. Instabilities cause many different geometry of the ablated micro-channel.

ACKNOWLEDGMENTS

This work received supported from the Capes, CNPq and Fapesp. We acknowledge cooperation with Cristina Kurachi.

REFERENCES

1. R. F. Z. Lizarelli, M. M. Costa, E. Carvalho Filho, F. D. Nunes, and V. S. Bagnato, Laser Phys. Lett. **5**, 63 (2008).
2. G. Nicolodelli, C. Kurachi, and V. S. Bagnato, Appl. Surf. Sci. **257**, 2419 (2011).
3. H. Ullah, M. Atif, S. Firdous, M. S. Mehmood, M. Ikram, C. Kurachi, C. Grecco, G. Nicolodelli, and V. S. Bagnato, Laser Phys. Lett. **7**, 889 (2010).
4. A. Z. Freitas, L. R. Freschi, R. E. Samad, D. M. Zezell, S. C. Gouw-Soares, and N. D. Vieira, Jr., Laser Phys. Lett. **7**, 236 (2010).
5. A. A. Ionin, S. I. Kudryashov, K. E. Mikhin, L. V. Seleznev, and D. V. Sinitsyn, Laser Phys. **20**, 1778 (2010).
6. H. Lao, H. Zhu, and X. Chen, Laser Phys. **20**, 245 (2010).
7. M. Zhou, E. L. Zhao, H. F. Yang, A. H. Gong, J. K. Di, and Z. J. Zhang, Laser Phys. **19**, 1470 (2009).
8. T. C. Chong, M. H. Hong, and L. P. Shi, Laser Photon. Rev. **4**, 123 (2010).
9. J. S. Fossa, M. R. B. Andreeta, and A. C. Hernandes, Laser Phys. **19**, 2045 (2009).
10. S. Klimentov, P. Pivovarov, V. Konov, D. Walter, M. Kraus, and F. Dausinger, Laser Phys. **19**, 1282 (2009).
11. V. M. Gordienko, I. A. Makarov, A. S. Khomenko, M. A. Timofeev, and V. V. Tuchin, Laser Phys. **19**, 1288 (2009).
12. V. I. Mazhukin, A. V. Mazhukin, and M. G. Lobok, Laser Phys. **19**, 1169 (2009).
13. A. V. Kabashin, Laser Phys. **19**, 1136 (2009).
14. D. Kawamura, A. Takita, Y. Hayasaki, and N. Nishida, Appl. Phys. A **85**, 39 (2006).
15. A. Zoubir, C. Lopez, M. Richardson, and K. Richardson, Opt. Lett. **29**, 1840 (2004).
16. D. N. Vitek, D. E. Adams, A. Johnson, P. S. Tsai, S. Backus, C. G. Durfee, D. Kleinfeld, and J. A. Squier, Opt. Express **18**, 18086 (2010).
17. R. R. Gattass, L. R. Cerami, and E. Mazur, Opt. Express **14**, 5279 (2006).
18. G. L. DesAutels, C. D. Brewer, M. A. Walker, S. B. Juhl, M. A. Finet, and P. E. Powers, Opt. Express **15**, 3139 (2007).
19. L. Ding, D. Jani, J. Linhardt, J. F. Künzler, S. Pawar, G. Labenski, T. Smith, and W. H. Knox, Opt. Express **16**, 21914 (2008).
20. S. Sowa, W. Watanabe, J. Nishii, and K. Itoh, Appl. Phys. A **81**, 1587 (2005).
21. S. Baudach, J. Bonse, J. Kruger, and W. Kautek, Appl. Surf. Sci. **154–155**, 555 (2000).
22. A. A. Serafetinides, M. Makropoulou, E. Fabrikes, E. Spyratou, C. Bacharis, R. R. Thomson, and A. K. Kar, Appl. Phys. A **93**, 111 (2008).
23. H. F. Yang, M. Zhou, J. K. Di, E. L. Zhao, and A. H. Gong, Laser Phys. **19**, 473 (2009).
24. D. Day and M. Gu, Opt. Express **13**, 5939 (2005).
25. B. H. Christensen and P. Balling, Phys. Rev. B **79**, 155424 (2009).
26. T. Perhavec, A. Gorkic, D. Bracun, and J. Diaci, Opt. Laser Technol. **41**, 397 (2009).
27. S. Rajesh and Y. Bellouard, Opt. Express **18**, 21490 (2010).
28. F. Canestri, J. Clin. Laser Med. Surg. **20**, 335 (2002).